# The Identification of Geological Samples Using Single Reflection Diamond ATR FTIR



Figure 1. The features of the Meridian™ accessory make it ideally suited to the analysis of geological samples.
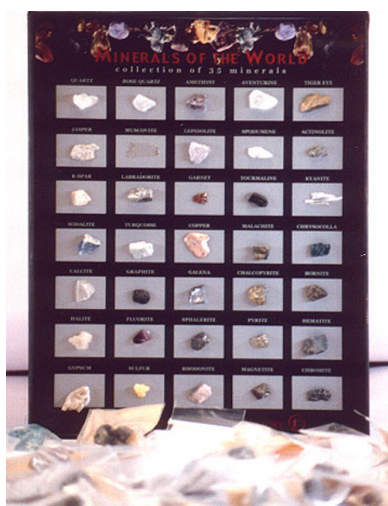


Figure 2. Samples were obtained from different sources along with identifications that were presumed reliable.

**ABSTRACT**

The advent of the micro-sampling single reflection ATR accessory as an adjunct to the FTIR spectrometer has made possible the analysis of many hard samples. The small sampling area, combined with calibrated pressure application on the sample, has allowed the acquisition of repeatable high quality spectra on samples which were previously intractable to the potent internal reflection technique. Recent developments have allowed the use of a monolithic natural diamond as the ATR element in such equipment so that now even the hardest samples may be analyzed without risk of damaging the strong and scratch-resistant internal reflection material.

The Harrick Scientific Meridian™ accessory has allowed the acquisition of spectra from mineral specimens. A variety of identified samples has been obtained from different, presumed reliable sources. Comparisons are made between spectra from different samples of the same mineral. In some cases, the results precipitate further investigation which is added to the discussion.

A discussion is given on the sample preparation technique. The preferred approach is to grind the samples to a very fine consistency prior to analysis, rather than attempt direct analysis on the intact solid. The effect of particle size and particle uniformity on absorbance level and repeatability is also presented.

The phenomena which contribute to the ATR spectra of powdered geological samples are summarized.

Finally, a discussion is given on the limitations of this technique, as well as some areas for future work. The selection of reliable sources, refining the sample preparation technique, and the effect of dispersion are included.

**OBJECTIVE**

The purpose of this work was to investigate the capabilities and limitations of the single reflection diamond ATR technique in the identification of geological samples.

**ID OF GEOLOGICAL SAMPLES USING SINGLE REFLECTION DIAMOND ATR FTIR**      **NO. 10204**

## EXPERIMENTAL

All spectra were taken with a Nicolet Nexus™ 670 FTIR spectrometer equipped with a DTGS detector and a standard mid-IR beamsplitter and using Nicolet EZ Omnic™ 5.1 software. All spectra were run at 4000 to 400 $cm^{-1}$, 32 scans, and 4 $cm^{-1}$ resolution. The gain was set to 8. A background spectrum was taken prior to each sample spectrum. The purge input of the spectrometer was connected to dry nitrogen at 25 SCFH. The accessory used was a Harrick Meridian™ (diamond SplitPea™). The accessory includes a 40° angular mask installed in the diamond ATR cartridge, to remove subcritical light rays.

The standard calibrated pressure applicator (with a 0 to 2.5 kg scale, calibrated in 0.5kg units) and the standard powder holder were installed in the accessory. The purge input of the accessory was connected to the purge fitting inside the sample compartment of the spectrometer. The purge ears of the accessory (PermaPurge™) were extended to the beam ports of the sample compartment. In this manner, samples could be run, one after the other, without breaking purge even with the sample compartment cover of the spectrometer open. See Figure 1. The monolithic (natural type 2A) diamond ATR element has sufficient strength to handle repeated measurements on mineral samples. Diamond, with a Mohs hardness of 10, is harder than the mineral specimens

Table 1: Hardness and refractive index for geological and ATR materials.

| Material | Formula | Refractive Index | Mohs Hardness |
|---|---|---|---|
| Actinolite | $Ca_2(Mg,Fe)_5Si_8O_{22}(OH)_2$ | 1.618-1.641 | 5-6 |
| Amethyst | $SiO_2$ | 1.54 | 7 |
| Bornite | $Cu_5FeS_4$ | ? | 3 |
| Calcite | $CaCO_3$ | 1.64 | 3 |
| Chalcopyrite | $CuFeS_2$ | ? | 3.5-4 |
| Chromite | $FeCr_2O_4$ | 2.1 | 5.5 |
| Chrysocolla | $CuSiO_3 \cdot nH_2O$ | 1.50 | 2-4 |
| Diamond | C | 2.4 | 10 |
| Flint | $SiO_2$ | 1.54 | 7 |
| Fluorite | $CaF_2$ | 1.43 | 4 |
| Galena | PbS | 4.0 | 2.5-2.7 |
| Germanium | Ge | 4.02 | 6 |
| Gypsum | $CaSO_4 \cdot 2H_2O$ | 1.52-1.53 | 2 |
| Halite | NaCl | 1.53 | 2 |
| Hematite | $Fe_2O_3$ | 2.9-3 | 6.5 |
| Iron Disulfide | $FeS_2$ | 1.81 | 6-6.5 |
| Iron(II,III)Oxide | $Fe_3O_4$ | 2.42 | 6 |
| Iron(III)Oxide | $Fe_2O_3$ | 2.9-3 | 6.5 |
| Jasper | $SiO_2$ | 1.54 | 7 |
| Kyanite | $Al_2SiO_3$ | 1.715-1.732 | 5-7 |
| Labradorite | $(Na,Ca)Al_{1-2}Si_{3-2}O_8$ | 1.565 | 6-6.5 |
| Lead Sulfide | PbS | 4.0 | 2.5-2.7 |
| Lepidolite | $K_2Li_3Al_4Si_7O_{21}(OH,F)_3$ | ? | 2.5-4 |
| Magnetite | $Fe_3O_4$ | 2.42 | 6 |
| Malachite | $Cu_2CO_3(OH)_2$ | 1.6-1.9 | 3.5-4 |
| Milky Quartz | $SiO_2$ | 1.54 | 7 |
| Onyx | $CaCO_3$ | 1.64 | 3 |
| Pyrite | $FeS_2$ | 1.81 | 6-6.5 |
| Rose Quartz | $SiO_2$ | 1.54 | 7 |
| Silicon | Si | 3.42 | 7 |
| Sodalite | $Na_4Al_3Si_3O_{12}Cl$ | 1.483 | 5.5-6 |
| Sphalerite | ZnS | 2.27 | 3.5-4 |
| Spodumene | $LiAlSi_2O_6$ | 1.65-1.68 | 6.5-7 |
| Tourmalene | $NaFe_3B_3Al_3(Al_3Si_6O_{27})(OH)_4$ | 1.63 | 7-7.5 |
| Tourquoise | $CuAl_6(PO_4)_4(OH)_8 \cdot 4H_2O$ | 1.61-1.65 | 5-6 |
| Zinc Selenide | ZnSe | 2.49 | 4 |
| Zinc Sulfide | ZnS | 2.27 | 3.5-40 |

Table 2: Sample and Reference Sources

| Sample Sources | Reference Material Sources |
| --- | --- |
| American Museum of Natural History<br>Central Park West at 79th Street<br>New York, NY 10024<br>(212) 769-5000 | Alfa Aesar<br>30 Bond Street<br>Ward Hill, MA 01835<br>(978) 521-6300 |
| Astro Gallery of Gems<br>185 Madison Avenue<br>New York, NY 10016<br>(212) 889-9000 | Fisher Scientific<br>711 Forbes Avenue<br>Pittsburgh, PA 15219<br>(412) 562-8300 |
| BMB Turquoise Corporation<br>P.O. Box 112<br>Gales Ferry, CT 06335<br>(860) 464-8078 | Harrick Scientific Products, Inc.<br>141 Tompkins Avenue, 2nd Floor<br>P.O. Box 277<br>Pleasantville, New York 10570<br>(914) 747-7202 |
| Minerals Unlimited<br>127 No. Downs<br>P.O. Box 877<br>Ridgecrest, CA 93556<br>(760) 375-5279 | |
| Oro Valley Gems<br>9755 N. Calle Buena Vista<br>Oro Valley, AZ 85737<br>(520) 544-5672 | |

selenide ATR element or zinc selenide refractive optics limit the longest wavelength to approximately $600 \text{ cm}^{-1}$. This limitation would block important features from the spectra of geological samples.

Finally, the diamond material of the ATR is very easy to clean. This feature is especially appreciated when a large number of samples have to be run. Geological sample and reference materials were obtained from numerous sources, listed in Table 2. Although the identifications provided by these sources were, at first, assumed to be reliable, this turned out to be incorrect in some cases, as will be discussed later in this report. See Figure 2.

The initial intention was to run all samples with little or no sample preparation. That is, other than reducing the sample to a thickness of 12mm or less (for compatibility with the unmodified accessory), no sample preparation was anticipated. It was found, however, that due to the irregular surface of most samples, spectra were difficult to obtain. Contact between the sample and the active surface of the ATR element could not be reliably achieved. For this reason alone, the solid sampling technique was rejected. Given the foreknowledge that some of the samples (e.g., halite, which is natural sodium chloride) would have no spectral features in the 4000 to $400 \text{ cm}^{-1}$ region, it was imperative that a sampling technique

chosen for this study, whose Mohs hardness is in the 2 ($CaSO_4 \cdot 2H_2O$, gypsum) to 7.5 ($NaFe_3B_3Al_3(Al_3Si_6O_{27})(OH)_4$, tourmalene) range. Diamond is, in fact, harder than all other mineral specimens which span from a Mohs hardness of 1 ($Mg_3Si_4O_{10}(OH)_2$, talc) to 9 ($Al_2O_3$, corundum or sapphire). With such a range, and assuming that the sample is unidentified, diamond becomes an imperative. All other ATR-suitable materials, including silicon, are softer than $Al_2O_3$, and cannot, therefore, be used for the

ATR element without the risk of damage. See Table 1.

The spectral range of the diamond ATR configuration and reflective transfer optics used in the Meridian™ ($45,000 \text{ cm}^{-1}$ to FIR) is more than adequate to cover the range of samples intended for this study. Spectra taken in this study were limited to the 4000 to $400 \text{ cm}^{-1}$ range by the spectrometer configuration available in our laboratory, not by the accessory. Alternate accessory designs which employ a composite diamond/zinc

---

be developed that would result in spectral features where such features were present. In one experiment, we were able to accumulate five spectra on different spots of a solid, homogeneous sample of jasper, a form of quartz. (To obtain these spectra, several runs, having poor contact, produced spectra with no peaks or peaks of very low absorbance. These spectra were discarded.) The spectra are shown in Figure 3. These spectra showed a large difference in absorbance levels, attributed to variation in the amount of contact with the ATR element. More importantly, they showed differences in spectral features, an effect attributed to various crystal orientations. This situation is obviously problematic for qualitative analysis based on single readings from standard references and unknowns. The same problem would exist for samples which are non-homogeneous chemically, as many geological samples are. In both cases, the single spot analyzed the solid with the ATR technique is not representative of the whole sample.

A sample preparation technique was developed which would quickly reduce a solid sample to a powder:

1. Use a cold chisel and/or hammer to produce pieces approximately 12mm on a side or less.

2. Place these pieces between two stainless steel plates and crush with a hammer.

3. Grind the resultant particles with a mortar and pestle until no larger particles are evident.

The procedure described above was used on all samples, except those reference materials obtained from a chemical supplier as pure substances, already ground to a fine consistency. Producing powders from solid samples was reduced to the consistency of fine sand. Approximately $60mm^3$ (the tip of a 6mm spatula) of a sample were then placed in the powder holder, the pressure applicator was applied to the 2.5kg mark, and the spectrum was taken.

Using the above procedure, three powder spectra were obtained on the same jasper sample. In this case, all spectra appear to have the same spectral

features, as seen in Figure 4, a minimum requirement for the qualitative analysis intended in this report. Variability in absorbance levels, although less than with the solid sample is still present, and will be discussed later in this report.

The pressure at the 2.5kg mark used with the pressure applicator is more than adequate for all the geological samples analyzed. Pressures at the 0.5, 1.0, 1.5, 2.0, and 2.5kg marks were exerted on two samples: calcite ($CaCO_3$), with a Mohs hardness of 3 and milky quartz ($SiO_2$), with a Mohs hardness of 7.

In all cases, there were no differences in absorbance levels attributable to the change in pressure. This apparent insensitivity to different pressures is attributed to the incompressible nature of the samples in question.

**RESULTS**

Quartz

Perhaps one of the most ubiquitous minerals is quartz ($SiO_2$). Several species of this mineral were analyzed: rose quartz, amethyst, jasper, flint, and milky quartz. All showed a characteristic pattern of peaks: 1085-1090 cm$^{-1}$ (moderate; antisymmetric Si-O-Si stretch), 797-798 cm$^{-1}$ and 778-780 cm$^{-1}$ (doublet, moderate-weak; Si-O stretch); 694-695 cm$^{-1}$ (weak; O-Si-O bend); and 456-465 cm$^{-1}$ (strong). The basic difference between these materials is in small impurities, called inclusions. These impurities substitute for the silicon atom in the crystal matrix, causing a color change in the visible region of the spectrum. Such color changes are obviously not detectable in the mid-infrared, nor are any significant differences seen in the mid-IR spectra of these species. Hence, it does not appear practical, from mid-IR FTIR spectroscopy alone, to distinguish between the various species of quartz. However, once the identification of quartz is made, an experienced mineralogist can probably identify which type is at hand simply by looking at the color. Figure 5 shows the spectra of the various species of quartz mentioned above. This figure also includes the spectrum of one sample, erroneously labeled "jasper" by one of the sources. This sample consisted, it is

believed, of small amounts of jasper in an as yet unknown matrix.

Calcium Carbonate

Two species of $CaCO_3$ were run, calcite and onyx. The sample set included two specimens of calcite from different sources. Their spectra are shown in Figure 6, showing an excellent match in spectral features. Three characteristic peaks are listed by Nakamoto[10] at 1429-1492, 879, and 706 $cm^{-1}$. The spectra obtained show a similar pattern with peaks at a slightly different 1414-1416 (moderate), 874 (moderate-weak), and 712 (weak). As with quartz, although it is not possible to distinguish these two materials based on the mid-IR spectrum alone, once $CaCO_3$ has been determined, it is relatively easy to distinguish between calcite and onyx by their different appearances.

Gypsum

Two samples of gypsum ($CaSO_4 \cdot H_2O$) from different sources were run. The spectra, showing a very good match, are depicted in Figure 7. The weak peaks at 1682 and 1620 $cm^{-1}$ and the strong to moderate peaks at 1114-1117, 668-669, and 599-600 $cm^{-1}$ are all attributed to the SO bond. Weak peaks at 3538-3544 $cm^{-1}$ and 3401 $cm^{-1}$, not shown, are both attributed to OH.

Kyanite

The spectra of two samples of kyanite ($Al_2SiO_5$) in Figure 8 show good correlation with moderate to weak peaks at 939, 567, 545, 506, 465-468, and 433-438 $cm^{-1}$, attributed to SiO and moderate to weak peaks at 727 and 671 $cm^{-1}$, attributed to AlO.

Malachite

This mineral ($Cu_2CO_3(OH)_2$) has a spectrum as rich as many organics. Three samples, shown in Figure 9, were run. Two were relatively pure malachite, and a very close correlation can be seen. The third sample was a mixture of small fragments of malachite in an unknown matrix. Weak peaks at 3399-3403 and 3308-3323 $cm^{-1}$, not shown, are attributed to OH. The moderate peak at 1493-1494 $cm^{-1}$ and the weak peak at 712 $cm^{-1}$ are attributed to CO. The remainder of the moderate to weak matching peaks has not yet been assigned.

Turquoise

Spectra for this mineral ($CuAl_6(PO_4)_4(OH)_8 \cdot 4H_2O$) are given in Figure 10. Three samples of relatively pure turquoise are shown with one sample which probably contains only small amounts
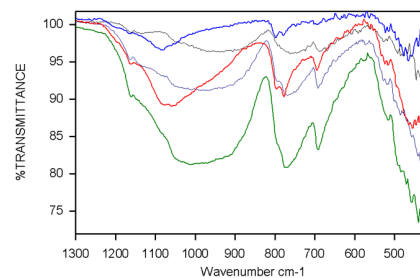


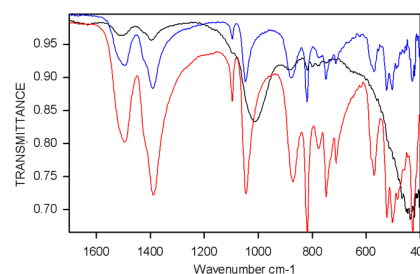Figure 3. Spectra taken of solid jasper samples showed different spectral characteristics.



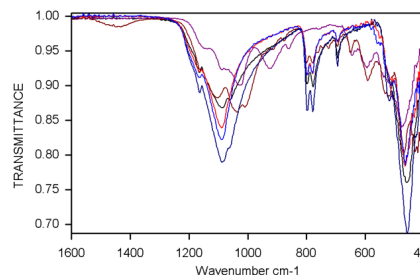Figure 4. Spectra taken of powdered jasper samples showed uniform spectral characteristics.



Figure 5. Spectra of various species of quartz ($SiO_2$), along with one spectrum of misidentified jasper. The spectra are from milky quartz (dark blue), flint (light blue), jasper (red), contaminated jasper (purple), amethyst (brown), and rose quartz (black).
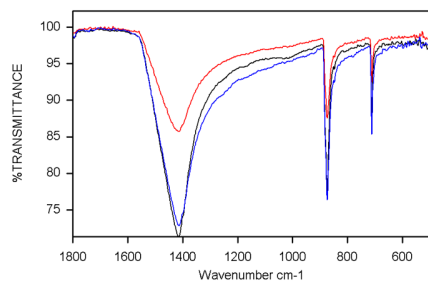
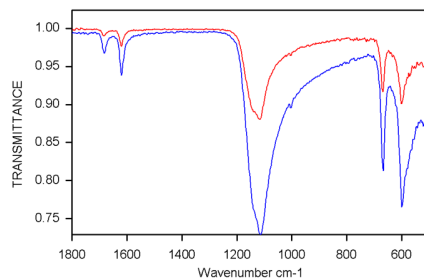Figure 6. Spectra of calcite (blue and red) and onyx (black), two species of calcium carbonate (CaCO3).
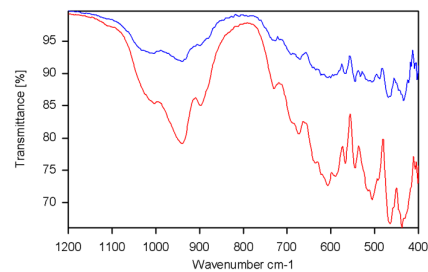


Figure 7. Spectra of two samples of gypsum ($CaSO_4 \cdot H_2O$).



Figure 8. Spectra of two samples of kyanite ($Al_2SiO_5$).



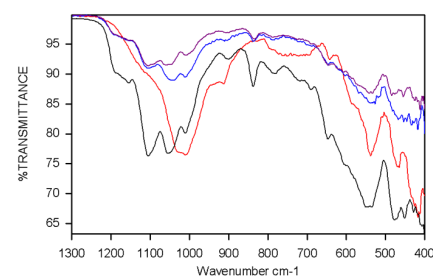Figure 10. Spectra of three samples of pure turquoise ($CuAl_6(PO_4)_4(OH)_8 \cdot 4H_2O$) and one sample of contaminated turquoise (red).
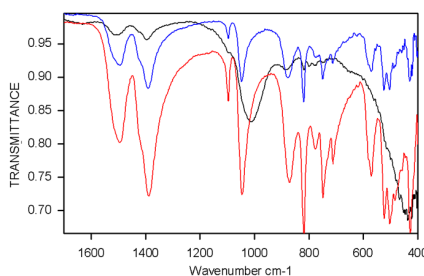


Figure 9. Spectra of two samples of pure malachite (red and blue), $Cu_2CO_3(OH)_2$, and one sample of contaminated malachite (black).



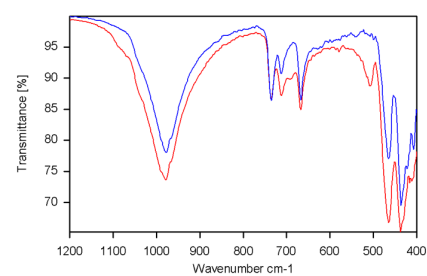Figure 11. Spectra of two samples of sodalite ($Na_4Al_3Si_3O_{12}Cl$).

of this expensive mineral in a matrix of unknown material.

As yet unassigned peaks at 1105, 1055-1058, and 834-837 cm$^{-1}$ are well matched between the three pure samples. Also matching are weak peaks, not shown, at approximately 3510 and 3465 cm$^{-1}$, attributed to OH.

### Sodalite

Sodalite ($Na_4Al_3Si_3O_{12}Cl$) spectra from two samples, shown in Figure 11, show excellent agreement, with the exception of two peaks, at 691 and 507 cm$^{-1}$, in one of the samples, possibly the result of an impurity. Good correlation is found in the moderate peak at 978-979cm$^{-1}$, the weak peaks at 735, 712, and 667-668 cm$^{-1}$, and the strong peaks at 465 and 436-437 cm$^{-1}$.

### Chromite

Two samples of this substance ($FeCr_2O_4$) were run, showing a fair match with moderate to weak peaks at

956-960, 631-646, and 443-448 cm$^{-1}$. See Figure 12.

### Spodumene

Figure 13 depicts spectra taken from two specimens of spodumene ($LiAlSi_2O_6$). There is a fair match with moderate to weak peaks at 1022-1028, 922-924, 644-645, 594 and 470-476 cm$^{-1}$.

### Actinolite

Actinolite ($Ca_2(Mg,Fe)5Si_8O_{22}(OH)_2$) spectra of two samples are given in Figure 14. Bands for OH, if present, were not observed. The weak peak of one sample at 1431cm$^{-1}$ may be an impurity. There is an otherwise good match between the two samples with moderate peaks at 950 and 919 cm$^{-1}$, weak peaks at 757-758, 683, and 666 cm$^{-1}$, and a strong peak at 441-445 cm$^{-1}$.

### Iron Disulfide
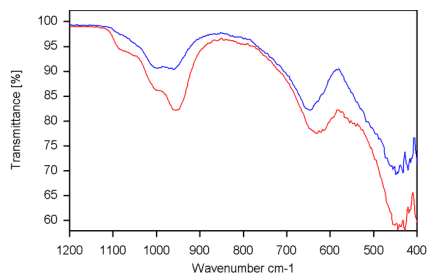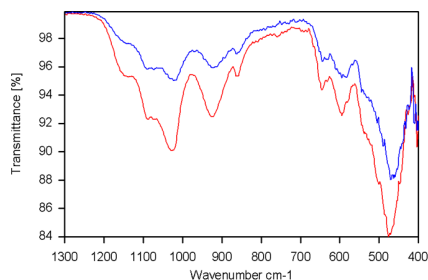
Figure 12. Spectra of two samples of chromite ($FeCrO_4$).



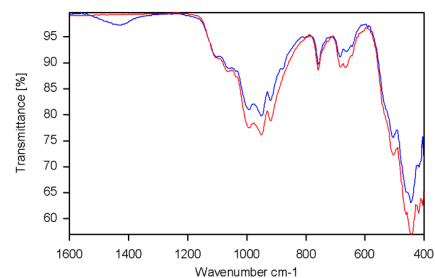Figure 13. Spectra of two samples of spodumene ($LiAlSi_2O_6$).



Figure 14. Spectra of two samples of actinolite

The spectra for two samples of iron disulfide ($FeS_2$) are shown in Figure 15. One sample is a mineral specimen of pyrite, ground as described in the experimental section of this report. The other sample is reference material, supplied at a −100 mesh granulation, from Alpha Aesar (30 Bond Street, Ward Hill, MA 01835). Both spectra show a peak at 411 $cm^{-1}$. Also, both spectra show a curious inverted peak at 440 $cm^{-1}$, which may be attributed to reflection at a wavelength where the refractive index of the sample is very high (i.e., higher than the bulk refractive index of 1.8)

Halite
Spectra from two samples of halite (NaCl), given in Figure 16, exhibit the expected near 100% flat transmission line. One of the samples has an unidentified impurity which manifested as two peaks at 1130 and 617 $cm^{-1}$. The peak at 336 $cm^{-1}$, listed by Nakamoto[10], was not accessible to the spectrometer equipment available in this study.

Miscellaneous
Several additional spectra, not shown in this report, were acquired for the following minerals: fluorite ($CaF_2$), sphalerite (ZnS), bornite ($CuFeS_4$), galena (PbS), hematite ($Fe_2O_3$), magnetite ($Fe_3O_4$), chalcopyrite ($CuFeS_2$), lepidolite ($K_2Li_3Al_4Si_7O_{21}(OH,F)_3$), labradorite (($Na,Ca)Al_{1-2}Si_{3-2}O_8$), tourmaline (black-schorl) ($NaFe_3B_3Al_3(Al_3Si_6O_{27})(OH)_4$), and chrysocolla ($CuSiO_3·2H_2O$). With these spectra, there was poor correlation between different sources of the

same mineral, the spectral features were too weak to make concrete comparisons, or the samples appeared to be mixed with interfering impurities.

DISCUSSION
The single reflection diamond ATR technique shows significant promise as a tool for geological analysis. Representative samples may be rapidly prepared. No special skills are required in obtaining spectra on these samples. No special algorithms are required for interpreting the results. Although many samples (e.g., halite, or NaCl) require FIR spectrometer capability for full spectra there are also many samples which characteristic peaks in the 4000 to 400 $cm^{-1}$ region. In fact, most of the spectral information obtained in this study was concentrated in the 1500 to 400 $cm^{-1}$ region. Spectral features in this area are enhanced by ATR, since the effective pathlength is proportional to wavelength. While the steel plates used to prepare the samples were scratched and nicked by the process, the diamond ATR element, after all samples were analyzed, remained undamaged.

Not all geological samples can be positively identified using this technique alone. One example highlighted in this report is quartz, with its variety of different species. However, this methodology can serve as a powerful adjunct to existing methodologies: chemical analysis, hardness testing, refractive index matching, x-ray crystallography, simple observation, etc.

A few problematic areas were noted in the course of this work. One area of current limitation is in

literature sources for spectroscopic identification. (See Figure 17 and the Reference section.) Only one text could be found which dealt with functional infrared identification of inorganic substances. Further work is required in researching the basic literature and in building a special purpose library.

A second limiting area is that a number of different sources for the same mineral must be obtained in building any library. This is to protect the library from misidentified or contaminated samples. (Obviously, the ultimate goal is to be able to analyze the composition of mixed samples. However, the first step is to obtain spectra of samples of pure compounds.) Wherever possible, the sample spectra should be compared with spectra obtained from pure reference material. For such simple samples as $FeS_2$, this is practical. However, most geological samples are quite complex, and one cannot obtaina pure reference sample from any chemical supplier. For example, it is not possible to order reagent grade powder for turquoise which has a chemical formula of $CuAl_6(PO_4)_4(OH)_8 \cdot 4H_2O$.

A third limitation is that certain geological samples do not have a consistent chemical formula, even though each individual sample would be considered "pure." For example, labradorite consists of a mixture of $NaAlSi_3O_8$ and $CaAl_2Si_2O_8$, in which the composition of any valid sample may be 50 to 70% of the latter chemical. The garnets and tourmalines are additional examples. Obviously, for such cases, a larger set of previously analyzed samples, covering the whole composition range, would be required. A fourth area is the device itself. The present powder cup/pressure applicator design is shown in Figure 18.

Here the powder cup, also serving as a liquid reservoir, has an O-ring seal at the bottom. When running many samples, as in this study, cleaning of the cup is required between each sample. Here, the O-ring, although not required by this application, must be cleaned. Also, with the cup geometry, set up to accommodate the conical tip of the pressure applicator, the minimum amount of sample required is not foolproof. (One wishes to use sufficient sample so that back reflection from the pressure applicator is ruled out.) A new, yet to be tested design, also shown in Figure 18, is exclusively for powders. This configuration eliminates the unneeded O-ring in the cup. The cup also has a cylindrical reservoir which should be filled to the top, thereby assuring sufficient sample between the ATR element and the pressure applicator tip. The new tip is also cylindrical, to match the cup. The performance of this design will be evaluated in a subsequent report.
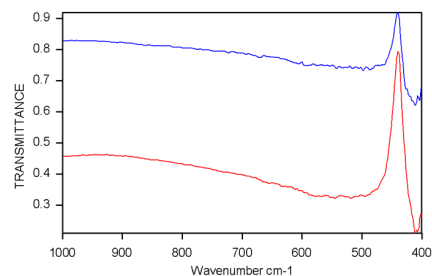


Figure 15. Spectra of two samples of iron disulfide ($FeS_2$): pyrite (blue) and reference material (red).
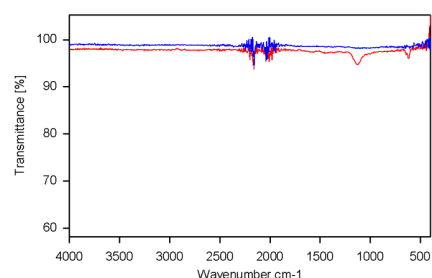


Figure 16. Spectra of two samples of halite (NaCl).



Figure 17. Although there are many texts dealing with rocks and minerals, there are few dealing with inorganic FTIR analysis.

The fifth area is sample preparation. Before discussing this specifically, we should first discuss some of the complex optical factors effecting the spectra obtained in this study. First is the expected interaction of light with the sample at the point of internal reflection. Second, distortions due to dispersion, especially apparent with peaks evidencing intense absorbance, are caused by high refractive indices of the sample, ones which cause an increase in the apparent critical angle. The consequences of such distortions are offset, at least somewhat, by the use of the same equipment configuration for both known standards and unknowns to be identified. Third, with samples of high refractive index, it is also possible to get some degree of simple reflection of light off the sample, without other interaction. The inverted peak for $FeS_2$, shown in Figure 15, may be evidence of this. Fourth, one cannot rule out scattering effects with powders. Fifth and perhaps the dominant factor involved in this study is optical contact between the powder sample and the active ATR surface. Strictly speaking, such "contact" is the presence of sample in the volume dp (penetration depth) deep above the ATR surface. Where the sample does not fill this volume, total internal reflection will occur without all of the light interacting with the sample. That is, such a volume will be a source of stray light and the resultant distortion in absorbance. Peak intensities and the signal to noise ratio will be reduced. This last optical factor is extremely dependent on sample preparation. An inspection of the majority of peaks obtained in this study indicated that typical absorbances were well under 0.1A, seemingly too small.

Further indirect evidence was obtained when samples such as sphalerite (ZnS), a zinc sulfide reference sample, and a zinc selenide reference sample, all with refractive indices close to that of diamond and all prepared as described in the experimental section, all had spectra whose plateau areas were at 90% transmission, or greater. In the spectra for $FeS_2$, the plateau %T dropped significantly in going from the experimentally prepared powder sample (at an estimated mesh size of −30 to −40, as explained below) to the reference material at −100 mesh. Finally, a reference sample of $Fe_3O_4$, received at a −325 mesh size and not otherwise processed, which has a refractive index of 2.4 (identical to diamond), produced a spectrum whose plateau transmission was in the 25 to 55% range. Such a "dark" reading is what would be expected of a sample whose refractive index matched the ATR element. As seen in Table 3, the particle size of this sample was 44 microns and under. A microscope examination of one milky quartz sample (using RAPP Polymere 250-315 micron polystyrene beads for comparison) indicated a wide range for samples prepared by the procedure outlined
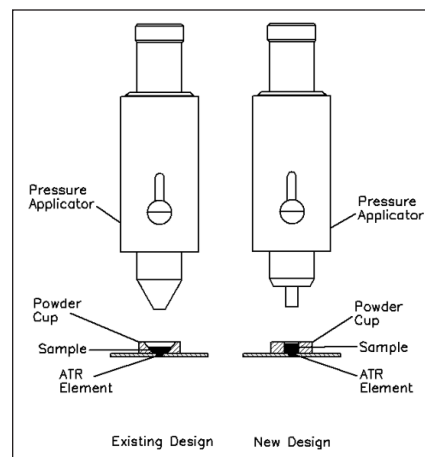


Figure 18. Existing and proposed new designs for powder compression applicator/cup for Meridian™ and SplitPea™ accessories.

Table 3: Mesh size conversion table.

| Mesh Size | Approximate Micron |
| --- | --- |
| 16 | 1190 |
| 20 | 840 |
| 30 | 590 |
| 40 | 420 |
| 50 | 297 |
| 60 | 250 |
| 70 | 210 |
| 80 | 177 |
| 100 | 149 |
| 150 | 104 |
| 200 | 74 |
| 230 | 62 |
| 270 | 53 |
| 325 | 44 |
| 400 | 37 |
| 500 | 25 |

Note: Mesh sizes less than 16, although readily available, are not pertinent to this study. The mesh size of 500 may be a practical limit, as the 635 mesh size is very expensive. Mesh sizes greater than 635 are not readily available.

in the experimental section: from a few microns to 500 microns. That is, our sample preparation technique produced an effective mesh size of only −30 to -40. Five samples of this milky quartz sample were run, and produced, after baseline correction, an absorbance of 0.067A at the 1083-1088 $cm^{-1}$ peak, with a relative standard deviation of 36%. Using a 325 mesh (McMaster-Carr part number 9319T45), it was found that only 8% by weight of the milky quartz sample was at −325 mesh. That is, 92% of the sample had a particle size greater than 44 microns. Additional processing of the original sample was then done to run 5 samples of the −325 mesh milky quartz. Now the absorbances at the 1083-1088 $cm^{-1}$ peak were 0.132A +/- 6.7%. Hence, with a reduction in the size of the particle size, the spectral contrast increased by a factor of two and the variability decreased by a factor of 0.2. Another interesting observation is that, in going to the smaller particle size, there was a small peak wavelength shift toward shorter wavelengths. As a result of this article size reduction, the sample was reduced from a consistency of fine sand to that of plaster of paris.

The reason why particle size has such a dramatic effect on absorbance is relatively straightforward. Smaller particles will more effectively fill the active volume of the ATR element, with fewer stray light "holes," resulting in higher absorbances. Likewise the effect on reproducibility is easily explained. Smaller particles, with a tighter range of sizes, will present a more homogeneous set of samples to the ATR element, hence reproducibility will increase. Note that, with the Meridian™ accessory, the active ATR spot is only 500microns. A larger spot size would be less susceptible to effects of particle size range on reproducibility. The wavelength shift explanation is more problematic. Obviously, additional work is required to determine the optimum mesh size, to improve (speed up) the sample preparation necessary to obtain that size, and to verify, investigate, and explain the wavelength shift phenomenon.

**REFERENCES**

1. Alfa Aesar Catalog, 2001-2002, Alfa Aesar, 30 Bond Street, Ward Hill, MA 01835.
2. Amethyst Galleries, Inc., Dublin, OH, mineral. galleries.com.
3. Argus International, Ltd., Santa Cruz, CA, www. argusinternational.com
4. S. S. Ballard, K. A. McCarthy, W. L. Wolfe, *Optical Materials for Infrared Instrumentation*, University of Michigan Willow Run Laboratories, Ann Arbor 1959.
5. N. B. Colthup, L.H. Daly, and S.E. Wiberly, *Introduction to Infrared and Raman Spectroscopy*, 2nd ed., Academic Press, New York (1975).
6. N. J. Harrick: *Internal Reflection Spectroscopy*, Harrick Scientific Corp., Ossining, New York 1987.
7. Harrick Scientific Products, Pleasantville, NY.
8. McMaster-Carr Supply Company Catalog 102, McMaster-Carr Supply Company, 473 Ridge Road, Dayton, New Jersey 08810.
9. The Mineralogical Society, London, www.minersoc.org.
10. K. Nakamoto: *Infrared and Raman Spectroscopy of Inorganic and Coordination Compounds, Part A: Theory and Applications in Inorganic Chemistry*, 5th ed., J. Wiley & Sons, New York 1997.
11. R. M. Pearl: *How to Know the Minerals and Rocks*, The New American Library 1959.
12. R. M. Pearl: *Rocks and Minerals*, Barnes & Noble 1963.
13. F. H. Pough: *A Field Guide to Rocks and Minerals*, 3rd ed., Houghton Mifflin Company, Boston 1960.
14. *Rock & Gem* 29(7), (1999).
15. *Rock & Gem* 31(8), (2001).
16. University of Wisconsin, Department of Geology and Geophysics, Madison, WI, www.geology.wisc.edu.
17. R. C. Weast (ed.): *Handbook of Chemistry and Physics*, 47th ed., The Chemical Rubber Co., Cleveland 1966.
18. H. S. Zim, P. R. Shaffer: *Rocks and Minerals*, Golden Press, New York 1957.
19. S. Zulver: *Rocks and Minerals*, Ottenheimer Publishers, New York 1963.